

Regional differences of chemical composition and optical properties of aerosols in the Tibetan Plateau

Jianzhong Xu¹, Anusha Priyadarshani Silva Hettiyadura², Yanmei Liu¹, Xinghua Zhang¹,
Shichang Kang¹, Julia Laskin², Alexander Laskin²

¹State Key Laboratory Cryospheric Sciences, Northwest Institute of Eco-Environment and Resources, Chinese Academy of Science, Lanzhou 730000, China

²Department of Chemistry, Purdue University, West Lafayette, Indiana 47907-2084, United States

Contents of this file

Figures S1 to S5

Tables S1

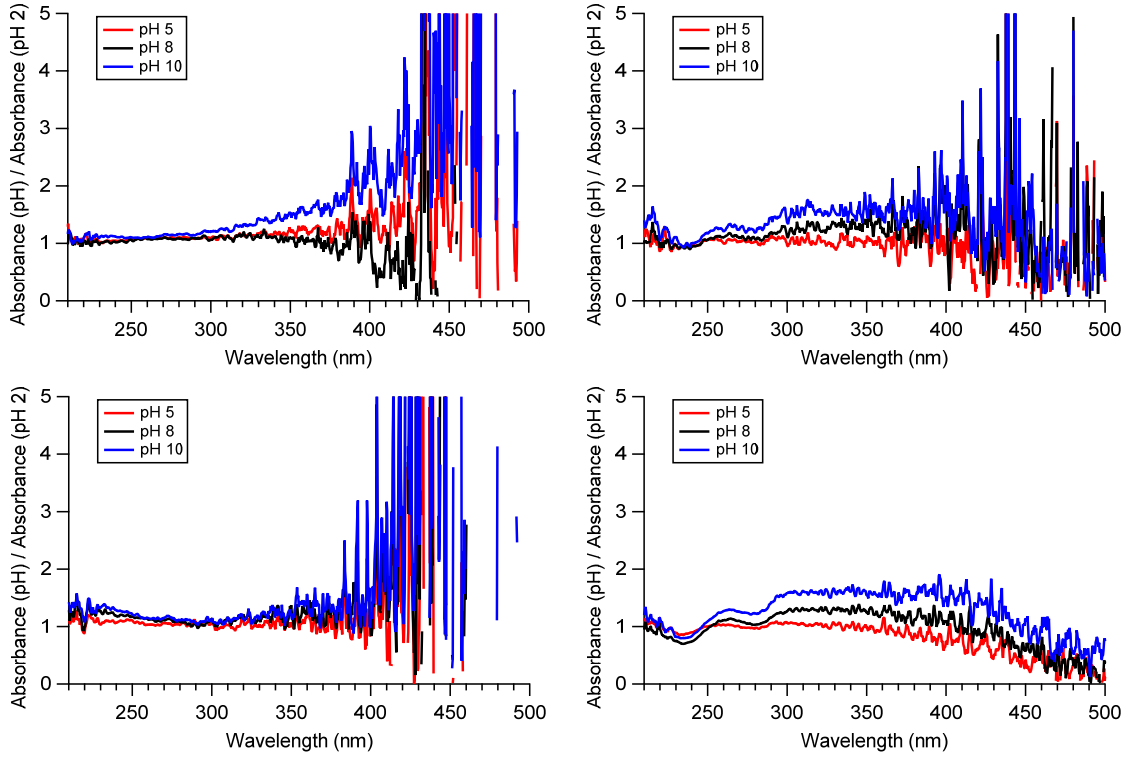


Figure S1. The average absorption spectra at pH 5, 8, and 10 normalized to absorption at pH2.

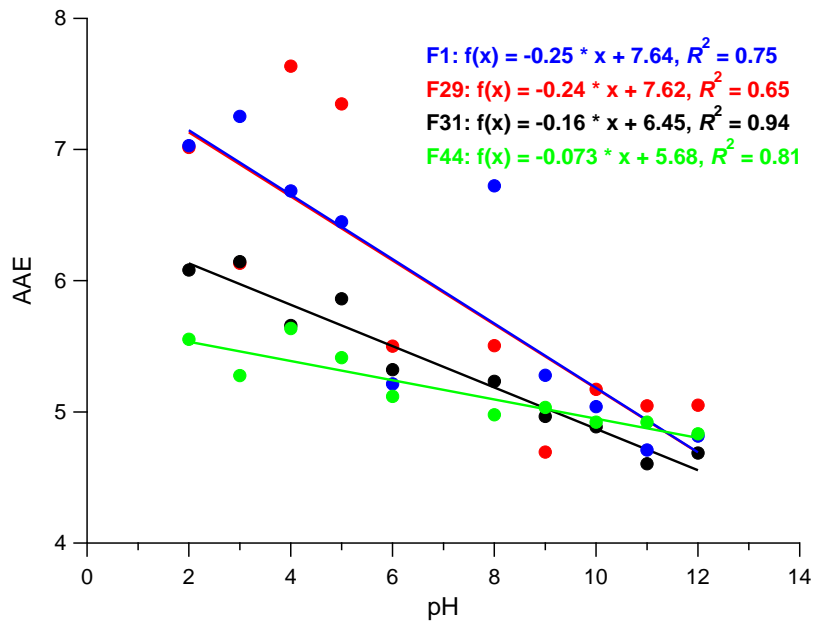


Figure S2. The AAE (absorption angstrom exponent) as a function of pH for samples at QOMS.

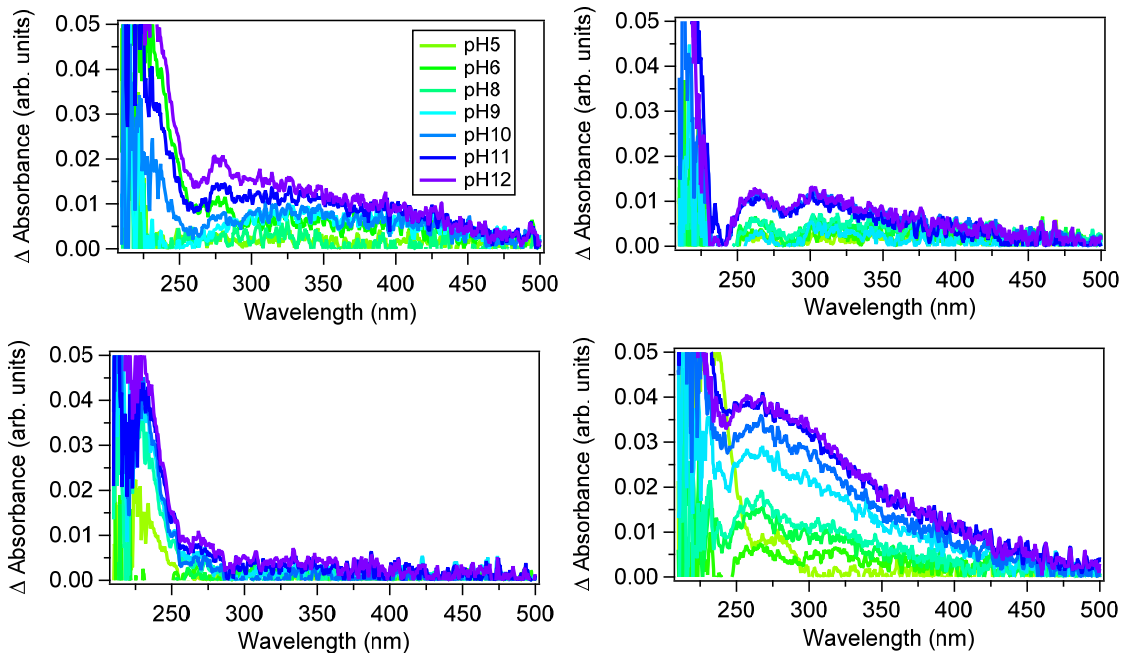


Figure S3. The absorption at a particular pH value with reference to pH2

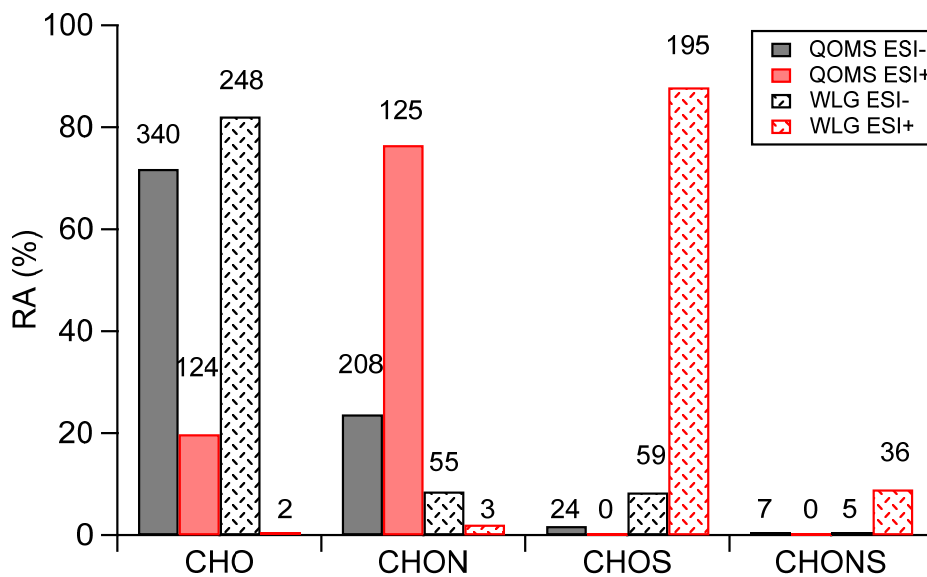


Figure S4. The relative abundance (RA) of each formula category in each site (QOMS; solid color, WLG; patterned fill) detected in either ESI+ (red) or ESI- (black) modes. The number of formulas detected are indicated above each column.

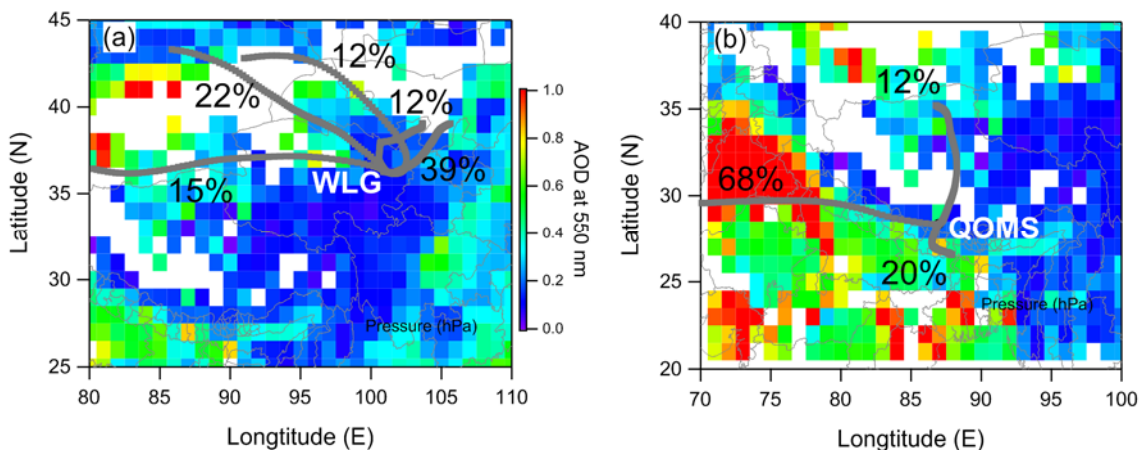


Figure S5. MODIS AOD around the sampling site during the field campaign and clusters of air mass back trajectories for (a) WLG and (b) QOMS. The air mass back trajectory analysis using the HYSPLIT model and the trajectories were recovered back to 72h at a 1h interval from the sampling sites at about 1000 m above ground level using a 1° resolution Global Data Assimilation System (GDAS) dataset. The cluster analysis for these trajectories was completed based on the directions of the trajectories.

Table S1. The sampling information for each filter at two sites.

Sampling Site	Filter Name	Sampling at beginning	Sampling date ending	Sampling duration	Sampling volume (m ³)	Mass conc. (µg m ⁻³)
QOMS, (28.36° N, 86.95° E, 4276 m a.s.l)	F1	04/13/2016 08:15	04/15/2016 08:00	47h45min	47.8	18.4
	F13	04/15/2016 08:25	04/17/2016 08:00	47h35min	47.7	7.73
	F14	04/17/2016 08:15	04/19/2016 08:00	47h45min	47.8	6.46
	F15	04/19/2016 08:15	04/21/2016 08:00	47h45min	47.8	2.78
	F28	04/21/2016 08:30	04/23/2016 08:00	47h30min	47.6	7.26
	F29	04/23/2016 08:15	04/25/2016 08:00	47h45min	47.8	6.43
	F30	04/25/2016 08:15	04/27/2016 08:00	47h45min	47.8	n.d.
	F31	04/27/2016 08:15	04/29/2016 08:00	47h45min	47.8	12.5

	F43	04/29/2016 08:15	05/01/2016 08:00	47h45min	47.8	n.d.
	F44	05/01/2016 08:15	05/03/2016 08:00	47h45min	47.8	7.51
	F45	05/03/2016 08:15	05/05/2016 08:00	47h45min	47.8	6.26
	F58	05/05/2016 08:50	05/07/2016 08:00	47h10min	47.3	1.99
	F59	05/07/2016 08:15	05/08/2016 21:43	37h28min	37.5	n.d.
	F60	05/09/2016 08:15	05/11/2016 08:00	47h45min	47.8	1.74
	F61	05/11/2016 08:15	05/13/2016 08:00	47h45min	47.8	1.87
	Blank 1	04/21/2016 08:05	04/21/2016 08:20	15min	/	/
	Blank 2	05/05/2016 08:05	05/05/2016 08:15	10min	/	/
	Blank 3	05/13/2016 09:46	05/13/2016 09:56	10min	/	/
WLG (36.28° N, 100.9° E, 3816 m a.s.l)	F1	06/29/2017 08:05	07/01/2017 07:45	47h40min	47.8	14.4
	F2	07/01/2017 08:05	07/03/2017 07:45	47h40min	47.8	11.4
	F3	07/03/2017 08:05	07/05/2017 07:45	47h40min	47.8	7.6
	F4	07/05/2017 08:05	07/07/2017 07:45	47h40min	47.8	15.6
	F5	07/07/2017 08:05	07/09/2017 07:45	47h40min	47.8	9.6
	F6	07/07/2017 08:05	07/09/2017 07:45	47h40min	47.8	5.9
	F7	07/09/2017 08:05	07/11/2017 07:45	47h40min	47.8	7.4
	F8	07/11/2017 08:05	07/13/2017 07:45	47h40min	47.8	10.6
	F9	07/13/2017 08:05	07/15/2017 07:45	47h40min	47.8	16.2
	F10	07/15/2017 08:05	07/17/2017 07:45	47h40min	47.8	18.6
	F11	07/17/2017 08:05	07/19/2017 07:45	47h40min	47.8	n.d.

F12	07/19/2017 08:05	07/21/2017 07:45	47h40min	47.8	n.d.
F13	07/21/2017 08:05	07/23/2017 07:45	47h40min	47.8	18.3
F14	07/23/2017 08:05	07/25/2017 07:45	47h40min	47.8	10.6
F15	07/25/2017 08:05	07/27/2017 07:45	47h40min	47.8	3.0
F16	07/27/2017 08:05	07/29/2017 07:45	47h40min	47.8	7.1
Blank 1	06/29/2017 07:50	06/29/2017 08:00	10min	/	/
Blank 2	07/09/2017 07:50	07/09/2017 08:00	10min	/	/